LETTER

doi:10.1038/nature25027

# MicroRNAs from the parasitic plant *Cuscuta campestris* target host messenger RNAs

Saima Shahid[1,2], Gunjune Kim[3], Nathan R. Johnson[1,2], Eric Wafula[2], Feng Wang[1,2]†, Ceyda Coruh[1,2]†, Vivian Bernal-Galeano[3], Tamia Phifer[4], Claude W. dePamphilis[1,2], James H. Westwood[3] & Michael J. Axtell[1,2]

**Dodders (*Cuscuta* spp.) are obligate parasitic plants that obtain water and nutrients from the stems of host plants via specialized feeding structures called haustoria. Dodder haustoria facilitate bidirectional movement of viruses, proteins and mRNAs between host and parasite[1], but the functional effects of these movements are not known. Here we show that *Cuscuta campestris* haustoria accumulate high levels of many novel microRNAs (miRNAs) while parasitizing *Arabidopsis thaliana*. Many of these miRNAs are 22 nucleotides in length. Plant miRNAs of this length are uncommon, and are associated with amplification of target silencing through secondary short interfering RNA (siRNA) production[2]. Several *A. thaliana* mRNAs are targeted by 22-nucleotide *C. campestris* miRNAs during parasitism, resulting in mRNA cleavage, secondary siRNA production, and decreased mRNA accumulation. Hosts with mutations in two of the loci that encode target mRNAs supported significantly higher growth of *C. campestris*. The same miRNAs that are expressed and active when *C. campestris* parasitizes *A. thaliana* are also expressed and active when it infects *Nicotiana benthamiana*. Homologues of target mRNAs from many other plant species also contain the predicted target sites for the induced *C. campestris* miRNAs. These data show that *C. campestris* miRNAs act as trans-species regulators of host-gene expression, and suggest that they may act as virulence factors during parasitism.**

In host-induced gene silencing (HIGS), siRNA-producing transgenes silence targeted pathogen and parasite mRNAs in *trans*[3,4]. Plant-based HIGS is effective against fungi[5], nematodes[6], insects[7] and the parasitic plant *Cuscuta pentagona*[8]. The ease with which HIGS can be introduced into plants suggests that they might exchange naturally occurring small RNAs with parasites. Consistent with this hypothesis, small RNAs from the plant pathogenic fungus *Botrytis cinerea* target host mRNAs during infection[9], and HIGS targeting of dicer-like mRNAs in *B. cinerea* reduces pathogen virulence[10]. Conversely, host miRNAs are exported from cotton into the fungal pathogen *Verticillium dahliae*[11]. However, to our knowledge, no examples of naturally occurring trans-species miRNAs have been described for plant–plant interactions.

*Cuscuta* haustoria facilitate bidirectional movement of viruses, proteins, and mRNAs[1], but the functional effects of these movements are unclear. *Cuscuta* is susceptible to HIGS, so we hypothesized that naturally occurring small RNAs might be exchanged across the *C. campestris* haustorium and affect gene expression in the recipient species. We profiled small-RNA expression in *C. campestris* grown on *A. thaliana* hosts using high-throughput small-RNA sequencing (small-RNA-seq). Two biological replicates each from three tissues were analysed: parasite stem, comprising a section of *C. campestris* stem above the site of haustorium formation; interface, comprising *C. campestris* stem with haustoria with associated *A. thaliana* stem tissue; and host stem, comprising sections of *A. thaliana* stems above the interface region, as previously described[12]. Small-RNA-producing loci from both organisms were identified, classified, and subjected to differential-expression analyses (Supplementary Data 1).

As expected, owing to dilution of parasite RNA with host RNA, *C. campestris* small-RNA loci were generally downregulated in the interface relative to the parasite stem (Fig. 1a). However, 76 *C. campestris* small-RNA species were significantly upregulated in the interface relative to the parasite stem (false discovery rate (FDR) $\leq$0.05). Of these interface-enriched species, 43 (57%) were miRNA species with canonical accumulation of discrete miRNA–miRNA* pairs (the expected processing intermediates of miRNA biogenesis) from

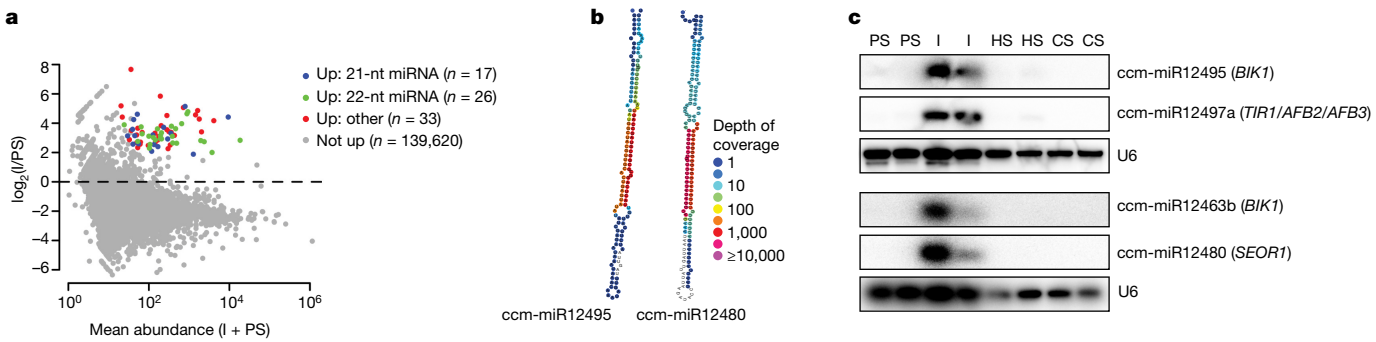


**Figure 1 | *C. campestris* miRNAs induced at the haustorial interface.** **a**, Mean abundance plot of *C. campestris* small-RNA loci comparing interface (I) to parasite stem (PS). Significantly upregulated (Up) loci are highlighted (alternative hypothesis: true difference > 2-fold, FDR $\leq$ 0.05 after Benjamini–Hochberg correction for multiple testing). nt, nucleotide. **b**, Predicted secondary structures of induced *C. campestris* miRNA hairpin precursors with colour-coded small-RNA-seq coverage per nucleotide. **c**, RNA blots of 22-nucleotide interface-induced miRNAs. HS, host stem; CS, control stem. U6, small nuclear RNA loading control. The experiment was performed twice with similar results. Full gels are shown in Supplementary Fig. 1.

[1]Huck Institutes of the Life Sciences, The Pennsylvania State University, University Park, Pennsylvania 16802, USA. [2]Department of Biology, The Pennsylvania State University, University Park, Pennsylvania 16802, USA. [3]Department of Plant Pathology, Physiology and Weed Science, Virginia Polytechnic Institute and State University, Blacksburg, Virginia 24061, USA. [4]Knox College, Galesburg, Illinois 61401, USA. †Present addresses: Department of Biology, Indiana University, Bloomington, Indiana 47405, USA (F.W.); Salk Institute for Biological Studies, La Jolla, California 92037, USA (C.C.).

predicted stem–loop precursors (Fig. 1b, Supplementary Data 2–4). RNA blots confirmed interface-specific expression of specific miRNAs (Fig. 1c). One of the 43 miRNAs is a member of the conserved *MIR164* family; the other 42 upregulated miRNAs have low sequence similarity to known miRNA loci, and none of the mature miRNAs or miRNA* aligned perfectly with the *A. thaliana* genome (Supplementary Data 5). Several of the miRNA loci were detected by PCR of *C. campestris* genomic DNA prepared from four-day old seedlings that had never interacted with a host plant (Extended Data Fig. 1). The majority of the induced *C. campestris* miRNAs (26 out of 43) produced a 22-nucleotide mature miRNA. Such 22-nucleotide miRNAs occur less frequently than 21-nucleotide miRNAs in plants, and they are strongly associated with accumulation of secondary siRNA from their targets[13,14]. Secondary siRNAs are thought to amplify miRNA-directed gene silencing[2].

We hypothesized that the induced 22-nucleotide miRNAs would cause formation of secondary siRNA from targeted host mRNAs. Therefore, we searched small-RNA-seq data for *A. thaliana* mRNAs that both contained plausible miRNA-complementary sites and shared sequences with siRNAs that accumulated specifically at the interface. Six *A. thaliana* mRNAs were found that met both criteria: *TIR1*, *AFB2* and *AFB3*, which encode partially redundant auxin receptors[15]; *BIK1*, which encodes a plasma-membrane-localized kinase required for both pathogen-induced and developmental signalling[16,17]; *SEOR1*, which encodes an abundant phloem protein that reduces photosynthate loss from the phloem after injury[18,19]; and *HSFB4* (also known as *SCZ*), which encodes a predicted transcriptional repressor that is required for the formation of ground-tissue stem cells in roots[20–22]. The siRNAs produced from these mRNAs resembled other examples of secondary siRNAs in their size distributions, double-stranded accumulation, and phasing (Fig. 2a, b, Extended Data Fig. 2). *TIR1*, *AFB2* and *AFB3* are also known to be targeted by the 22-nucleotide miRNA miR393, and to produce secondary siRNAs downstream of the miR393-complementary site[23]. In parasitized stems, the location and phase register of the *TIR1*, *AFB2* and *AFB3* secondary siRNAs shift upstream, proximal to the sites that are complementary to the *C. campestris* miRNAs (Extended Data Fig. 2), implying that the *C. campestris* miRNAs, and not miR393, are triggering the interface-specific secondary siRNAs. The predominant 21-nucleotide phase register at several loci was shifted by +1 to +2 nucleotides relative to predictions. This is consistent with the 'phase drift' seen at other phased siRNA loci[24,25] that cause the register to be shifted forward, and is probably due to the presence of low levels of 22-nucleotide siRNAs. Analysis of uncapped mRNA fragments showed strong evidence for miRNA-directed cleavage at all of the sites complementary to *C. campestris* miRNAs, specifically those from interface samples but not from control stem samples (Fig. 2, Extended Data Fig. 2). We did not find any induced miRNAs or siRNAs from the *A. thaliana* host that were capable of targeting these six mRNAs. We also did not find any endogenous *C. campestris* secondary siRNA loci corresponding to any of the induced miRNAs. Some *C. campestris* orthologues of *TIR1, HSFB4* and *BIK1* had possible, but very poorly complementary, miRNA target sites (Extended Data Fig. 3). These observations suggest that the induced *C. campestris* miRNAs have evolved to avoid targeting 'self' transcripts. We conclude that 22-nucleotide miRNAs from *C. campestris* act in a trans-species manner to target *A. thaliana* mRNAs.

Accumulation of five of the six targets was significantly reduced in parasitized stems compared to control stems (Fig. 3a). The true magnitude of repression of these targets could be even greater, since many miRNAs also direct translational repression. Accumulation of *A. thaliana* secondary siRNAs is partially dependent on the endonuclease DCL4 (DICER-LIKE 4) and wholly dependent on RDR6 (RNA-DEPENDENT RNA POLYMERASE 6, also known as SGS2 or SDE1)[2]. Accumulation of an abundant secondary siRNA from *TIR1* was eliminated entirely in the *sgs2-1* mutant, and reduced in the *dcl4-2t* mutant (Fig. 3b). Thus, host *DCL4* and *RDR6* are required for secondary siRNA production. This implies that the *C. campestris*-derived miRNAs are

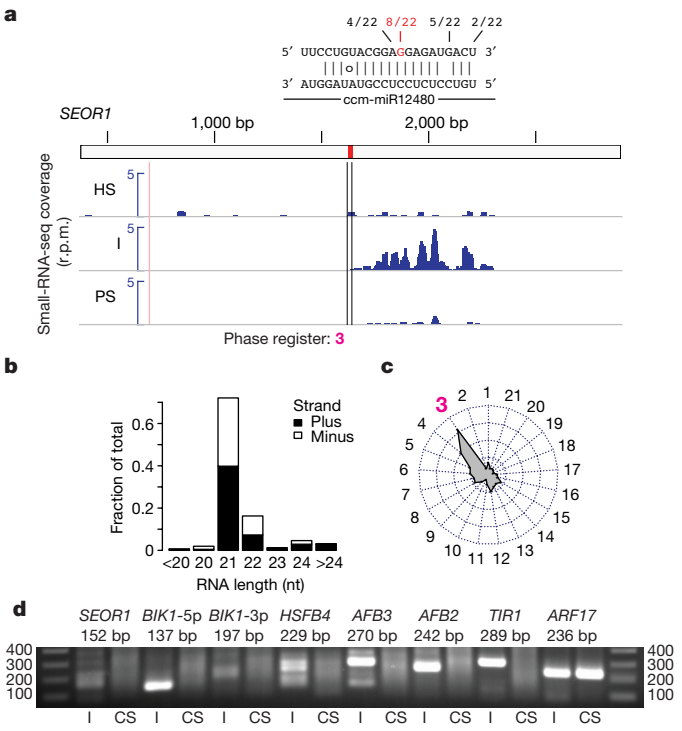


**Figure 2 | *C. campestris* miRNAs cause slicing and phased siRNA production from host mRNAs. a**, Small-RNA-seq coverage for *A. thaliana SEOR1* for host stem, interface and parasite stem. $n = 2$ biologically independent samples each; miRNA-complementarity is shown by RNA-ligase-mediated 5′-rapid amplification of cDNA ends (5′-RLM-RACE) and expected phase register; r.p.m., reads per million. **b**, Length and polarity distribution of *SEOR1*-mapped siRNAs from interface samples. **c**, Radar chart showing fraction of interface-derived siRNAs in each possible 21-nucleotide phasing register. **d**, 5′-RLM-RACE products from nested amplifications. *ARF17*, positive control. The experiment was performed once. Full gels are shown in Supplementary Fig. 1.

active inside host cells and hijack the host's own silencing machinery to produce secondary siRNAs.

In repeated trials, we did not observe consistent significant differences in parasite fresh weight using *dcl4-2t* and *sgs2-1* mutants as hosts (Extended Data Fig. 4). Thus, loss of induced secondary siRNAs is not sufficient to affect parasite growth in this assay. Similarly, there were no significant differences in biomass of *C. campestris* grown on *scz2* or *tir1-1/afb2-3*-mutant hosts (Fig. 3c). Significantly less ($P < 0.05$) *C. campestris* biomass was observed using the *bik1* mutant as host (Fig. 3c). However, interpretation of this result was complicated by the weak, frequently lodging stems of the *bik1* mutant[16]. *BIK1* is involved in both plant development and immunity, and its developmental functions may mask its role in the *C. campestris* interaction. Significantly more ($P < 0.05$) *C. campestris* biomass was observed on *seor1* or *afb3–4* mutants (Fig. 3c). Therefore, both *SEOR1* and *AFB3* function to restrict *C. campestris* growth on *A. thaliana*. This observation is consistent with the hypothesis that both *SEOR1* and *AFB3* are trans-species miRNA targets of biological relevance in *A. thaliana*.

*C. campestris* has a broad host range among eudicots[26]. Therefore, we searched for sites in eudicot orthologues of the targeted *A. thaliana* mRNAs that were complementary to the *C. campestris* miRNAs induced specifically at the interface. Probable orthologues of *BIK1, SEOR1, TIR1* and *HSFB4* were identified as predicted targets of interface-induced miRNAs in many eudicot species, while only one species had predicted targets in the orthologues of the negative control *GAPDH* (Fig. 4a, Extended Data Table 1). We conclude that the induced *C. campestris* miRNAs would be able to collectively target *TIR1, SEOR1, HSFB4* and *BIK1* orthologues in many eudicot species.

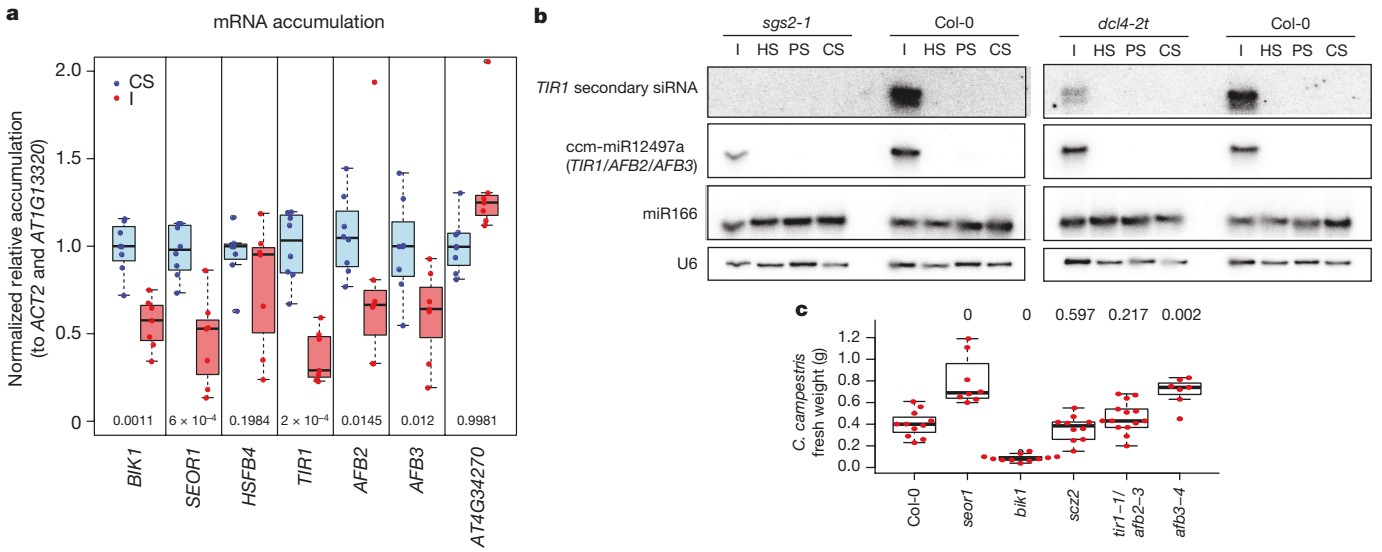


**Figure 3 | Effects of *C. campestris* miRNAs and their targets.** **a**, Accumulation of *A. thaliana* mRNA in interface versus control stems, shown by quantitative reverse-transcriptase polymerase chain reaction (qRT–PCR). Control stems, $n = 8$; interface, $n = 7$ biologically independent samples. Box plots show the median, box edges represent the first and third quartiles, and the whiskers extend to 1.5× interquartile range. *P* values are displayed above the *x* axis; Wilcoxon rank-sum tests, unpaired, one-tailed. *AT4G34270* (also known as TIP41-like protein), control. **b**, RNA blots from *C. campestris* infestations of the indicated *A. thaliana* genotypes. Full gels are shown in Supplementary Fig. 1. The experiment was performed twice with similar results. **c**, *C. campestris* biomass on *A. thaliana* hosts of the indicated genotypes. *P* values and plotting conventions as in **a**, except two-tailed tests were used; $n = 11$, 8, 11, 10, 14, and 7 biologically independent samples (left to right).

We performed additional small-RNA-seq from *C. campestris* on *A. thaliana* hosts, and from *C. campestris* on *N. benthamiana* hosts. Both sets of experiments were designed identically to the original small-RNA-seq study (two biological replicates each of host stem, interface and parasite stem samples). The interface-induced set of *C. campestris* miRNA loci was highly reproducible across both of the *A. thaliana* experiments as well as the *N. benthamiana* experiment (Extended Data Fig. 5). Induction of several *C. campestris* miRNAs during *N. benthamiana* parasitism was confirmed by RNA blots (Fig. 4b). Several *N. benthamiana* mRNAs both contained plausible target sites for *C. campestris* miRNAs and showed accumulation of phased, secondary siRNAs in the interface samples, including orthologues of *TIR1* and *BIK1* (Extended Data Fig. 6). Analysis of uncapped RNA ends provided strong evidence for miRNA-directed cleavage of one of the *N. benthamiana TIR1* orthologues (Fig. 4c, d). This is direct evidence that the same *C. campestris* miRNAs target orthologous host mRNAs in multiple species. None of the interface-induced miRNAs we tested were detectable in *C. campestris* pre-haustoria from seedling tips that had coiled around dead bamboo stakes instead of a live host (Fig. 4b, Extended Data Fig. 7). This suggests that contact with a living host is a requirement for expression of these miRNAs.

These data demonstrate that *C. campestris* induces a large number of miRNAs at the haustorium, and that some of these miRNAs target and reduce accumulation of host mRNAs. Many of the induced miRNAs are 22 nucleotides in length, and are associated with secondary siRNA production from their host targets using the host's secondary siRNA machinery. Several of the targets are linked to plant pathogenesis: manipulation of levels of *TIR1*, *AFB2*, and *AFB3* mRNA affects bacterial pathogenesis and defence signalling[27], and BIK1 is a central regulator of pathogen-induced signalling[28]. Perhaps the most intriguing target is *SEOR1*, which encodes a very abundant protein that is present in large agglomerations in phloem sieve-tube elements[18]. *seor1* mutants show an increased loss of sugars from detached leaves[19], and our data show that *seor1* mutants also support increased *C. campestris* growth. A key function of the haustorium is to capture nutrients from the host phloem; targeting *SEOR1* could be a strategy to increase sugar uptake from host phloem. Overall, these data suggest that *C. campestris* trans-species miRNAs might function as virulence factors to remodel host gene expression to the parasite's advantage. Further experiments that directly disrupt the delivery or function of these miRNAs will be needed to test this hypothesis directly.

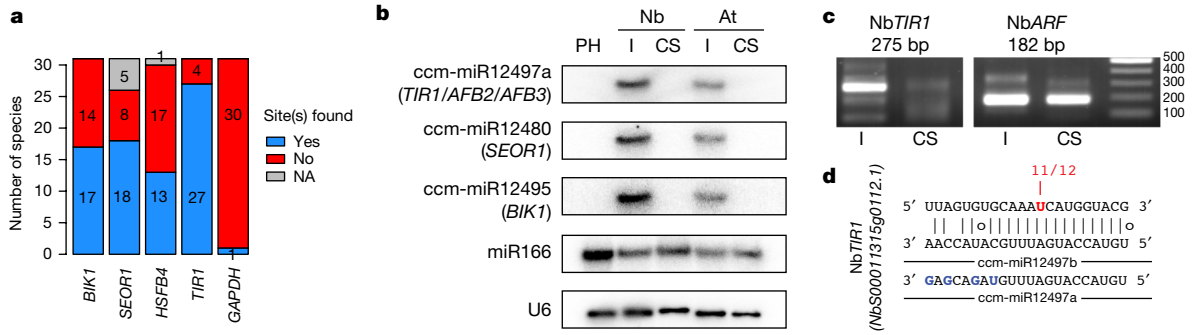


**Figure 4 | Conservation of host mRNA targeting by *C. campestris*.** **a**, Predicted targets of interface-induced *C. campestris* miRNA–miRNA*. NA, no orthologous genes found. **b**, RNA blots from interface and control stem of *C. campestris*-infested *N. benthamiana* (*Nb*), *A. thaliana* (*At*), and *C. campestris* pre-haustoria (PH). The experiment was performed once. **c**, 5′-RLM-RACE products for the indicated *N. benthamiana* cDNAs. *ARF*, positive control. The image was cropped to remove irrelevant lanes. Full gels are shown in Supplementary Fig. 1. The experiment was performed once. **d**, Complementary site and 5′-RLM-RACE results from a *N. benthamiana TIR1* orthologue.

**Online Content** Methods, along with any additional Extended Data display items and Source Data, are available in the online version of the paper; references unique to these sections appear only in the online paper.

**Received 26 September 2016; accepted 8 November 2017.**


1. Kim, G. & Westwood, J. H. Macromolecule exchange in *Cuscuta*–host plant interactions. *Curr. Opin. Plant Biol.* **26,** 20–25 (2015).
2. Fei, Q., Xia, R. & Meyers, B. C. Phased, secondary, small interfering RNAs in posttranscriptional regulatory networks. *Plant Cell* **25,** 2400–2415 (2013).
3. Baulcombe, D. C. VIGS, HIGS and FIGS: small RNA silencing in the interactions of viruses or filamentous organisms with their plant hosts. *Curr. Opin. Plant Biol.* **26,** 141–146 (2015).
4. Weiberg, A., Bellinger, M. & Jin, H. Conversations between kingdoms: small RNAs. *Curr. Opin. Biotechnol.* **32,** 207–215 (2015).
5. Nowara, D. *et al.* HIGS: host-induced gene silencing in the obligate biotrophic fungal pathogen *Blumeria graminis*. *Plant Cell* **22,** 3130–3141 (2010).
6. Huang, G., Allen, R., Davis, E. L., Baum, T. J. & Hussey, R. S. Engineering broad root-knot resistance in transgenic plants by RNAi silencing of a conserved and essential root-knot nematode parasitism gene. *Proc. Natl Acad. Sci. USA* **103,** 14302–14306 (2006).
7. Baum, J. A. *et al.* Control of coleopteran insect pests through RNA interference. *Nat. Biotechnol.* **25,** 1322–1326 (2007).
8. Alakonya, A. *et al.* Interspecific RNA interference of SHOOT MERISTEMLESS-like disrupts *Cuscuta pentagona* plant parasitism. *Plant Cell* **24,** 3153–3166 (2012).
9. Weiberg, A. *et al.* Fungal small RNAs suppress plant immunity by hijacking host RNA interference pathways. *Science* **342,** 118–123 (2013).
10. Wang, M. *et al.* Bidirectional cross-kingdom RNAi and fungal uptake of external RNAs confer plant protection. *Nat. Plants* **2,** 16151 (2016).
11. Zhang, T. *et al.* Cotton plants export microRNAs to inhibit virulence gene expression in a fungal pathogen. *Nat. Plants* **2,** 16153 (2016).
12. Kim, G., LeBlanc, M. L., Wafula, E. K., dePamphilis, C. W. & Westwood, J. H. Plant science. Genomic-scale exchange of mRNA between a parasitic plant and its hosts. *Science* **345,** 808–811 (2014).
13. Chen, H.-M. *et al.* 22-nucleotide RNAs trigger secondary siRNA biogenesis in plants. *Proc. Natl Acad. Sci. USA* **107,** 15269–15274 (2010).
14. Cuperus, J. T. *et al.* Unique functionality of 22-nt miRNAs in triggering RDR6-dependent siRNA biogenesis from target transcripts in *Arabidopsis*. *Nat. Struct. Mol. Biol.* **17,** 997–1003 (2010).
15. Dharmasiri, N. *et al.* Plant development is regulated by a family of auxin receptor F box proteins. *Dev. Cell* **9,** 109–119 (2005).
16. Veronese, P. *et al.* The membrane-anchored BOTRYTIS-INDUCED KINASE1 plays distinct roles in *Arabidopsis* resistance to necrotrophic and biotrophic pathogens. *Plant Cell* **18,** 257–273 (2006).
17. Lin, W. *et al.* Inverse modulation of plant immune and brassinosteroid signaling pathways by the receptor-like cytoplasmic kinase BIK1. *Proc. Natl Acad. Sci. USA* **110,** 12114–12119 (2013).
18. Froelich, D. R. *et al.* Phloem ultrastructure and pressure flow: Sieve-element-occlusion-related agglomerations do not affect translocation. *Plant Cell* **23,** 4428–4445 (2011).
19. Jekat, S. B. *et al.* P-proteins in *Arabidopsis* are heteromeric structures involved in rapid sieve tube sealing. *Front. Plant Sci.* **4,** 225 (2013).
20. Mylona, P., Linstead, P., Martienssen, R. & Dolan, L. SCHIZORIZA controls an asymmetric cell division and restricts epidermal identity in the *Arabidopsis* root. *Development* **129,** 4327–4334 (2002).
21. Pernas, M., Ryan, E. & Dolan, L. SCHIZORIZA controls tissue system complexity in plants. *Curr. Biol.* **20,** 818–823 (2010).
22. ten Hove, C. A. *et al.* SCHIZORIZA encodes a nuclear factor regulating asymmetry of stem cell divisions in the *Arabidopsis* root. *Curr. Biol.* **20,** 452–457 (2010).
23. Si-Ammour, A. *et al.* miR393 and secondary siRNAs regulate expression of the TIR1/AFB2 auxin receptor clade and auxin-related development of *Arabidopsis* leaves. *Plant Physiol.* **157,** 683–691 (2011).
24. Allen, E., Xie, Z., Gustafson, A. M. & Carrington, J. C. MicroRNA-directed phasing during trans-acting siRNA biogenesis in plants. *Cell* **121,** 207–221 (2005).
25. Axtell, M. J., Jan, C., Rajagopalan, R. & Bartel, D. P. A two-hit trigger for siRNA biogenesis in plants. *Cell* **127,** 565–577 (2006).
26. Dawson, J. H., Musselman, L. J., Wolswinkel, P. & Dörr, I. Biology and control of *Cuscuta*. *Rev. Weed Sci.* **6,** 265–317 (1994).
27. Robert-Seilaniantz, A. *et al.* The microRNA miR393 re-directs secondary metabolite biosynthesis away from camalexin and towards glucosinolates. *Plant J.* **67,** 218–231 (2011).
28. Lu, D. *et al.* A receptor-like cytoplasmic kinase, BIK1, associates with a flagellin receptor complex to initiate plant innate immunity. *Proc. Natl Acad. Sci. USA* **107,** 496–501 (2010).


**Supplementary Information** is available in the online version of the paper.

**Acknowledgements** This research was supported in part by awards from the US National Science Foundation (1238057 to J.H.W. and C.W.D.; 1339207 to M.J.A.) and the US National Institute of Food and Agriculture (135997 to J.H.W.).

**Author Contributions** S.S. and M.J.A. did the bioinformatics analysis. S.S., M.J.A. and N.R.J. prepared figures and tables. G.K., J.H.W., N.R.J., S.S., T.P. and M.J.A. cultivated and harvested plant specimens. E.W., G.K., C.W.D. and J.H.W. performed genome and transcriptome sequencing and assemblies. F.W., S.S. and N.R.J. did RNA blotting. S.S. and M.J.A. performed 5′-RLM-RACE and qRT–PCR. C.C. and T.P. constructed small-RNA-seq libraries. N.R.J. and V.B.-G. performed growth assays. M.J.A. and J.H.W. conceived the project. M.J.A. wrote and revised the manuscript.

**Author Information** Reprints and permissions information is available at www.nature.com/reprints. The authors declare no competing financial interests. Readers are welcome to comment on the online version of the paper. Publisher's note: Springer Nature remains neutral with regard to jurisdictional claims in published maps and institutional affiliations. Correspondence and requests for materials should be addressed to M.J.A. (mja18@psu.edu).

**Reviewer Information** *Nature* thanks M. Albert, F. Tang and the other anonymous reviewer(s) for their contribution to the peer review of this work.

## METHODS

*Cuscuta* was initially obtained from a tomato field in California, and seed stocks were derived from self-pollination through several generations in the Westwood laboratory. The isolate was initially previously identified as *Cuscuta pentagona*. *C. pentagona* is very closely related to *C. campestris*, and the two are distinguished by microscopic differences in floral morphology; because of this they have often been confused[29]. We subsequently determined that our isolate is indeed *C. campestris*. *A. thaliana sgs2-1* mutants[30] were a gift from H. Vaucheret (INRA Versailles). *A. thaliana dcl4-2t* mutants (GABI_160G05[31]) were obtained from the *Arabidopsis* Biological Resource Center (Ohio State University). *A. thaliana seor* mutants (GABI-KAT 609F04[18]) were a gift from M. Knoblauch (Washington State University). The *A. thaliana tir1-1/afb2-* and *afb3*-4 mutants[32] were a gift from G. Monshausen (Pennsylvania State University). The *bik1* mutant[16] was a gift from T. Mengiste (Purdue University). The *scz2* mutant[22] was a gift from R. Heidstra (Wageningen University). All *A. thaliana* mutants were on the Col-0 background.

**Growth conditions and RNA extractions.** For initial experiments (small-RNA-seq and RNA blots in Fig. 1), *A. thaliana* (Col-0) plants were grown in a growth room at 18–20 °C with 12 h light per day, illuminated (200 μmol $m^{-2}s^{-1}$) with metal-halide (400 W, GE multi-vapour lamp) and spot-gro (65 W, Sylvania) lamps. *C. campestris* seeds were scarified in concentrated sulfuric acid for 45 min, rinsed 5–6 times with distilled water and dried. The seeds were placed in potting medium at the base of four-week-old *A. thaliana* seedlings and allowed to germinate and attach to hosts. The *C. campestris* plants were allowed to grow and spread on host plants for an additional three weeks to generate a supply of uniform shoots for use in the experiment. Sections of *C. campestris* shoot tip (~10 cm long) were placed on the floral stems of a fresh set of *A. thaliana* plants. Parasite shoots coiled around the host stems and formed haustorial connections. Tissues from plants that had established *C. campestris* with at least two coils around healthy host stems and clear parasite growth were used in these studies. Control plants were grown under the same conditions as parasitized plants, but were not exposed to *C. campestris*.

For the preparation of tissue-specific small-RNA libraries, tissues were harvested after *C. campestris* cuttings had formed active haustorial connections to the host. This was evidenced by growth of the *C. campestris* shoot to a length of at least 10 cm beyond the region of host attachment (7–10 days after infection). Three tissues were harvested from the *A. thaliana*–*C. campestris* associations: 2.5 cm of *A. thaliana* stem above the region of attachment, *A. thaliana* and *C. campestris* stems in the region of attachment (referred to as the interface), 2.5 cm of the parasite stem near the point of attachment. To remove any possible cross-contamination between *A. thaliana* and *C. campestris*, harvested regions of the parasite and host stem were taken 1 cm away from the interface region and the surface of each harvested tissue cleaned by immersion for 5 min in 70% ethanol, the ethanol was decanted and replaced, the process was repeated three times and the stems were blotted dry with a Kimwipe after the final rinse. All three sections of tissue were harvested at the same time, and material from 20 attachments was pooled for small-RNA extraction. Small RNA was extracted from ~100 mg of each tissue using the mirPremier microRNA Isolation Kit (Sigma-Aldrich) according to the manufacturer's protocol. Small RNA was analysed using an small-RNA kit (Agilent) on a 2100 Bioanalyzer platform.

Samples used for 5′-RLM-RACE (Fig. 2d) and qRT–PCR (Fig. 3a) analyses of *A. thaliana* targets were prepared as described above with the following modifications: Col-0 *A. thaliana* hosts were cultivated in a growth room with 16-h days, 8-h nights, at ~23 °C under cool-white-fluorescent lamps. Attachment of *C. campestris* cuttings was promoted by illumination with far-red LED lighting for 3–5 days, and total RNA was extracted using Tri-reagent (Sigma) per the manufacturer's suggestions, followed by a second sodium-acetate–ethanol precipitation and wash step. Samples used for RNA blots of secondary siRNA accumulation from *A. thaliana* mutants and replicate small-RNA-seq libraries were obtained similarly, except that the samples were derived from the primary attachments of *C. campestris* seedlings on the hosts instead of from cuttings. In these experiments, scarified *C. campestris* seedlings were first germinated on moistened paper towels for three days at ~28 °C, then placed adjacent to the host plants with their radicles submerged in a water-filled 0.125-ml tube.

*C. campestris* pre-haustoria (Extended Data Fig. 7) were obtained by scarifying, germinating and placing seedlings as described above, next to bamboo stakes in soil, under illumination from cool-white fluorescent lights and far-red-emitting LEDs. Seedlings coiled and produced pre-haustoria four days after being placed, and were harvested and used for total-RNA extraction (used for RNA blots in Fig. 4b) using Tri-reagent as described above. *N. benthamiana* was grown in a growth room with 16-h days, 8-h nights, at ~23 °C, under cool-white fluorescent lamps. Three-to-four-week-old plants served as hosts for scarified and germinated *C. campestris* seedlings. Attachments were promoted by three-to-six days with supplementation by far-red-emitting LEDs. Under these conditions, *C. campestris* attached to the petioles, and not the stems, of the *N. benthamiana* hosts. Interfaces and control petioles from un-parasitized hosts were collected seven-to-eight days after successful attachments, and total RNA (used for RNA blots in Fig. 4b and small-RNA-seq libraries) was recovered using Tri-reagent as described above.

**Small-RNA-seq.** The initial small-RNA-seq libraries were constructed using the Tru-Seq small-RNA kit (Illumina) per the manufacturer's protocol and sequenced on an HiSeq2500 instrument (Illumina). Subsequent small-RNA-seq libraries (replicate two using *A. thaliana* hosts, and the *N. benthamiana* experiments) used the NEBnext small-RNA library kit (New England Biolabs), following the manufacturer's instructions. Raw small-RNA-seq reads were trimmed to remove 3′-adapters and filtered for quality and trimmed length ≥16 nucleotides using cutadapt[33] version 1.9.1 with the settings "-a TGGAATTCTCGGGTGCCAAGG–discard-untrimmed -m 16–max-n = 0". For experiments where *A. thaliana* was the host, trimmed reads that aligned with zero or one mismatch (using bowtie[34] version 1.1.2, settings "-v 1") to the *A. thaliana* plastid genome, the *Cuscuta gronovii* plastid genome (*C. gronovii* was the closest relative to *C. campestris* for which a completed plastid-genome assembly was publicly available), *A. thaliana* rRNAs, tRNAs, small nuclear RNAs (snRNAs), and small nucleolar RNAs (snoRNAs) were removed. Similarly, for experiments where *N. benthamiana* was the host, the reads were cleaned against the *C. gronovii* plastid genome, the *N. tabacum* plastid genome and rRNAs, and a set of tRNAs predicted from the *N. benthamiana* genome using tRNAscanSE.

For the original *A. thaliana* host data, the clean reads were aligned and analysed with reference to the combined TAIR10 *A. thaliana* reference genome and a preliminary version 0.1 draft genome assembly of *C. campestris* using ShortStack[35] (version 3.8.3) with default settings. The resulting annotated small-RNA loci (Supplementary Data 1) were analysed for differential expression (interface versus parasite stem) using DESeq2[36], with a $\log_2$ fold threshold of 1, alternative hypothesis of 'greaterAbs', and alpha of 0.05. *P* values were adjusted for multiple testing using the Benjamini–Hochberg procedure, and loci with an adjusted *P* value of ≤0.05 (equivalent to an FDR of ≤0.05) were denoted upregulated in interfaces relative to parasite stem. Among the upregulated loci, those annotated by ShortStack as miRNAs deriving from the *C. campestris* genome which produced either a 21- or 22-nucleotide mature miRNA (Supplementary Data 2) were retained and further analysed. The predicted secondary structures and observed small-RNA-seq read coverage was visualized (Supplementary Data 3, 4) using strucVis (version 0.3; https://github.com/MikeAxtell/strucVis).

For analysis of mRNA-derived secondary siRNAs, the clean small-RNA-seq reads from the original *A. thaliana* experiment were aligned to the combined TAIR10 representative cDNAs from *A. thaliana* and our preliminary version 0.1 transcriptome assembly for *C. campestris*, using ShortStack[35] v3.8.3, with the settings –mismatches 0,–nohp, and defining the full length of each mRNA as a locus using the option –locifile. The resulting counts of small-RNA alignments for each mRNA were used for differential-expression analysis, comparing interface to host stem, using DESeq2[36] as described above. *A. thaliana* mRNAs with significantly upregulated (FDR ≤0.05) small RNAs in the interface compared to host stem were retained for further analysis. The cDNA sequences of these loci were retrieved and used for miRNA target predictions using GSTAr (v1.0; https://github.com/MikeAxtell/GSTAr); the full set of mature miRNA and miRNA* (Supplementary Data 2) from the interface-induced *C. campestris* miRNA loci were used as queries.

Analysis of the second set of *A. thaliana*–*C. campestris* small-RNA-seq data aligned the cleaned reads to the combined *A. thaliana* and *C. campestris* reference genomes as described above, except that the list of loci derived in the analysis of the original data (Supplementary Data 1) was used as a –locifile in the ShortStack analysis. Differential-expression analysis was then performed using DESeq2 as described above. Analysis of the *N. benthamiana*–*C. campestris* small-RNA-seq data began with a ShortStack analysis of the cleaned reads against the combined *N. benthamiana* (v0.4.4) genome and the preliminary assembly of the *C. campestris* genome, using default settings. The *de novo N. benthamiana* loci obtained from this run were retained. The resulting alignments were used to quantify abundance of small RNAs from the *C. campestris* small-RNA loci defined with the original data. The resulting read counts were then used for differential-expression analysis with DESeq2 as described above. Analysis of secondary siRNAs derived from *N. benthamiana* mRNAs was performed in a similar way to the *A. thaliana* mRNA analysis described above, except that the combined transcriptomes were from *C. campestris* and *N. benthamiana* (v0.4.4 annotations).

**RNA blots.** Small RNA gel blots were performed as previously described[37] with modifications. For the blots shown in Fig. 1b, 1.8 μg of small RNA from each sample was separated on 15% TBE–Urea Precast gels (Bio-Rad), transblotted onto the Hybond NX membrane and cross-linked using 1-ethyl-3-(3-dimethylaminopropyl) carbodiimide[38]. Hybridization was carried out in 5× SSC, 2× Denhardt's solution, 20 mM sodium phosphate (pH 7.2), 7% SDS with 100 μg $ml^{-1}$ salmon testes DNA (Sigma-Aldrich). Probe labelling, hybridization and washing were performed as described[37]. Radioactive signals were detected using Typhoon FLA

7000 (GE Healthcare). Membranes were stripped between hybridizations by washing with 1% SDS for 15 min at 80 °C and exposed for at least 24 h to verify complete removal of probe before re-hybridization. Blots in Figs 3b and 4b were performed similarly, except that 12 μg of total RNA was used. Probe sequences are listed in Supplementary Data 6.

**5′-RNA ligase-mediated rapid amplification of cDNA ends.** Five micrograms total RNA was ligated to 1 μg of a 44-nucleotide RNA adaptor (Supplementary Data 6) using a 20 μl T4 RNA ligase 1 reaction (NEB) per the manufacturer's instructions for a 1 h incubation at 37 °C. The reaction was then diluted with 68 μl water and 2 μl 0.5 M EDTA pH 8.0, and incubated at 65 °C for 15 min to inactivate the ligase. Sodium acetate pH 5.2 was added to a final concentration of 0.3 M, and the RNA was precipitated with ethanol. The precipitated and washed RNA was resuspended in 10 μl water; 3.33 μl of this sample was used as template in a reverse transcription reaction using random primers and Protoscript II reverse transcriptase (NEB) per the manufacturer's instructions. The resulting cDNA was used as template in first round PCR using a 5′ primer matching the RNA adaptor and a 3′ gene-specific primer (Supplementary Data 6); 1 μl of the product was used as template for nested PCR with nested primers (Supplementary Data 6). Gene-specific primers for *A. thaliana* cDNAs were based on the representative TAIR10 transcript models, while those for *N. benthamiana* cDNAs were based on the v0.4.4 transcripts (Sol Genomics Network[39]). In Fig. 4c, *N. benthamiana TIR1* is transcript ID *NbS00011315g0112.1*; *N. benthamiana ARF* is transcript ID *NbS00059497g0003.1*. Bands were purified from agarose gels and cloned into pCR4-TOPO (Life Tech). Inserts from individual clones were recovered by colony PCR and analysed by Sanger sequencing.

**Quantitative reverse-transcription–PCR.** Total RNA used for qRT–PCR was first treated with DNaseI (RNase-free; NEB) per the manufacturer's instructions, ethanol precipitated and resuspended. The treated total RNA (2 μg) was used for cDNA synthesis using the High Capacity cDNA Synthesis Kit (Applied Biosystems) per the manufacturer's instructions. PCR reactions used PerfeCTa SYBR Green FastMix (Quantabio) on a StepONE-Plus quantitative PCR system (Applied Biosystems) per the manufacturer's instructions. Primers (Supplementary Data 6) were designed to span the miRNA target sites to ensure that only uncleaved mRNAs were measured. Three reference mRNAs were used: *ACT2*, *AT1G13320* (which encodes PDF2, a subunit of PP2A), and *AT4G34270*[40]. Raw $C_t$ values were used to calculate relative normalized expression values to each reference mRNA separately, and the final analysis used the median relative expression values between the *ACT12* and *AT4G34270*-normalized data.

***C. campestris* growth assays.** *C. campestris* seedlings were scarified, pre-germinated, and placed next to hosts in 0.125 ml water-filled tubes under cool-white fluorescent lighting supplemented with far-red-emitting LEDs (16-h day, 8-h night) at ~23 °C as described above. After a single attachment formed (four days), far-red light supplementation was removed to prevent secondary attachments. After 18 more days of growth, entire *C. campestris* vines were removed and weighed (Fig. 3c). Multiple additional growth trials were performed specifically on the *dcl4-2t* and *sgs2-1* mutant hosts under varying conditions (Extended Data Fig. 4).

**miRNA target predictions.** To find probable orthologues for *A. thaliana* genes of interest, the *A. thaliana* protein sequences were used as queries for a BLASTP analysis of the 31 eudicot proteomes available on Phytozome 11 (https://phytozome.jgi.doe.gov/pz/portal.html#). Transcript sequences for the top 100 hits were retrieved. In some cases no hits were found in a particular species; these are shown as 'NA' in Fig. 4a. The miRNA query set was all mature miRNA and miRNA* from the interface-induced, *C. campestris*-derived 21- or 22-nucleotide miRNAs (Supplementary Data 2). Probable targets from the 31 species were identified as those having a score of up to 4.5 using targetfinder.pl v0.1 (https://github.com/MikeAxtell/TargetFinder/).

*N. benthamiana* orthologues of *A. thaliana* proteins were found based on BLASTP searches against the v0.4.4 *N. benthamiana* protein models at Sol Genomics Network[39], and miRNA target sites predicted using targetfinder.pl as above.

**Statistics and reproducibility.** No statistical methods were used to predetermine sample size. The experiments were not randomized. 95% confidence intervals from Fig. 3a: 0.249 to 0.611 (*BIK1*), 0.267 to 0.781 (*SEOR1*), −0.122 to 0.649 (*HSFB4*), 0.385 to 0.894 (*TIR1*), 0.083 to 0.724 (*AFB2*), 0.071 to 0.678 (*AFB3*), −0.461 to −0.120 (*AT4G34270*). Note that these confidence intervals from unpaired Wilcoxon rank-sum tests are the estimators of the median of control stem minus interface for each gene. 95% confidence intervals from Fig. 3c: −0.580 to −0.200 (*seor1*), 0.220 to 0.400 (*bik1*), −0.070 to 0.150 (*scz2*), −0.170 to 0.060 (*tir1-1/afb2-3*), −0.440 to −0.180 (*afb3-4*). Note that these confidence intervals from unpaired Wilcoxon rank-sum tests are the estimators of the median of Col-0 minus the mutant for each comparison.

**Code availability.** ShortStack[35] (small-RNA-seq analysis), strucVis (visualization of predicted RNA secondary structures with overlaid small-RNA-seq depths), GSTAr.pl (prediction of miRNA targets) and Shuffler.pl/targetfinder.pl (prediction of miRNA targets controlling for false discovery rate) are all freely available at https://github.com/MikeAxtell. Cutadapt[33] is freely available at http://cutadapt.readthedocs.io/en/stable/index.html. The R package DESeq2[36] is freely available at http://www.bioconductor.org/packages/release/bioc/html/DESeq2.html.

**Data availability.** Small-RNA-seq data from this work are available at NCBI GEO under accession GSE84955 and NCBI SRA under project PRJNA408115. The draft, preliminary *C. campestris* genome and transcriptome assemblies used in this study are available at the Parasitic Plant Genome Project website at http://ppgp.huck.psu.edu. *C. campestris* miRNA loci have been registered with miRBase. Source data availability: Fig. 1b, in Supplementary Data 2 and 3; Figs 1c, 2c, d, 3b, 4b and c, in Supplementary Fig. 1; Fig. 3a, c and Extended Data Fig. 4, included as Source Data; Fig. 4a, in Extended Data Table 1. There are no restrictions on data availability and the corresponding author will provide any data not already included as Supplementary Data or as Source Data upon request.


29. Costea, M., García, M. A., Baute, K. & Stefanović, S. Entangled evolutionary history of *Cuscuta pentagona* clade: A story involving hybridization and Darwin in the Galapagos. *Taxon* **64,** 1225–1242 (2015).
30. Elmayan, T. *et al. Arabidopsis* mutants impaired in cosuppression. *Plant Cell* **10,** 1747–1758 (1998).
31. Xie, Z., Allen, E., Wilken, A. & Carrington, J. C. DICER-LIKE 4 functions in trans-acting small interfering RNA biogenesis and vegetative phase change in Arabidopsis thaliana. *Proc. Natl Acad. Sci. USA* **102,** 12984–12989 (2005).
32. Parry, G. *et al.* Complex regulation of the TIR1/AFB family of auxin receptors. *Proc. Natl Acad. Sci. USA* **106,** 22540–22545 (2009).
33. Martin, M. Cutadapt removes adapter sequences from high-throughput sequencing reads. *EMBnet. journal* **17,** 10–12 (2011).
34. Langmead, B., Trapnell, C., Pop, M. & Salzberg, S. L. Ultrafast and memory-efficient alignment of short DNA sequences to the human genome. *Genome Biol.* **10,** R25 (2009).
35. Johnson, N. R., Yeoh, J. M., Coruh, C. & Axtell, M. J. Improved placement of multi-mapping small RNAs. *G3 (Bethesda)* **6,** 2103–2111 (2016).
36. Love, M. I., Huber, W. & Anders, S. Moderated estimation of fold change and dispersion for RNA-seq data with DESeq2. *Genome Biol.* **15,** 550 (2014).
37. Cho, S. H., Coruh, C. & Axtell, M. J. miR156 and miR390 regulate tasiRNA accumulation and developmental timing in Physcomitrella patens. *Plant Cell* **24,** 4837–4849 (2012).
38. Pall, G. S. & Hamilton, A. J. Improved northern blot method for enhanced detection of small RNA. *Nat. Protoc.* **3,** 1077–1084 (2008).
39. Bombarely, A. *et al.* A draft genome sequence of *Nicotiana benthamiana* to enhance molecular plant–microbe biology research. *Mol. Plant Microbe Interact.* **25,** 1523–1530 (2012).
40. Czechowski, T., Stitt, M., Altmann, T., Udvardi, M. K. & Scheible, W.-R. Genome-wide identification and testing of superior reference genes for transcript normalization in *Arabidopsis*. *Plant Physiol.* **139,** 5–17 (2005).

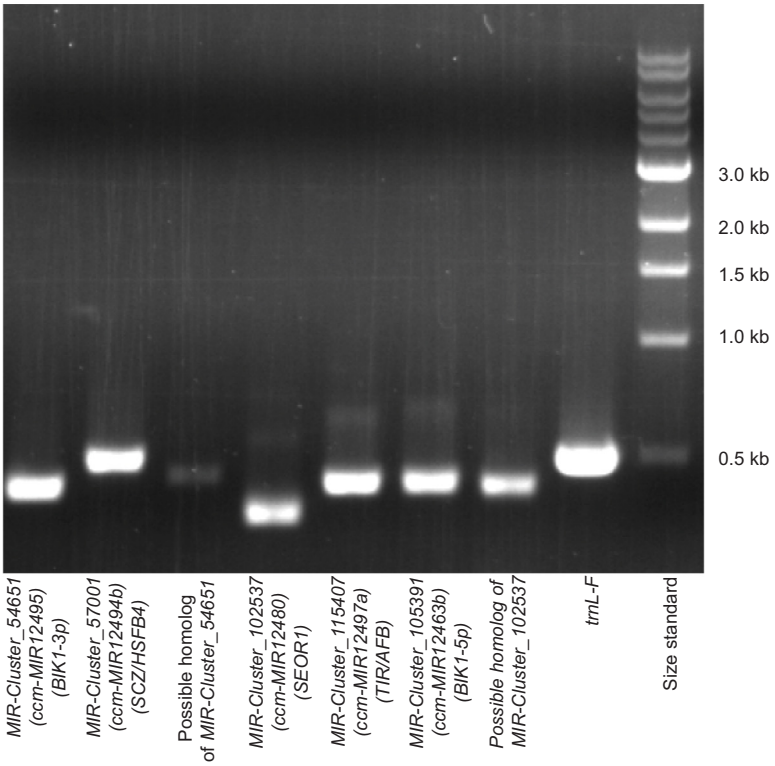


**Extended Data Figure 1 | PCR of *C. campestris* miRNA loci.** Genomic DNA isolated from *C. campestris* seedlings four days after germination was used as template; the seedlings had never attached to nor been near a host plant, ruling out host DNA contamination. *trnL-F*, positive control plastid locus. Experiment performed once.

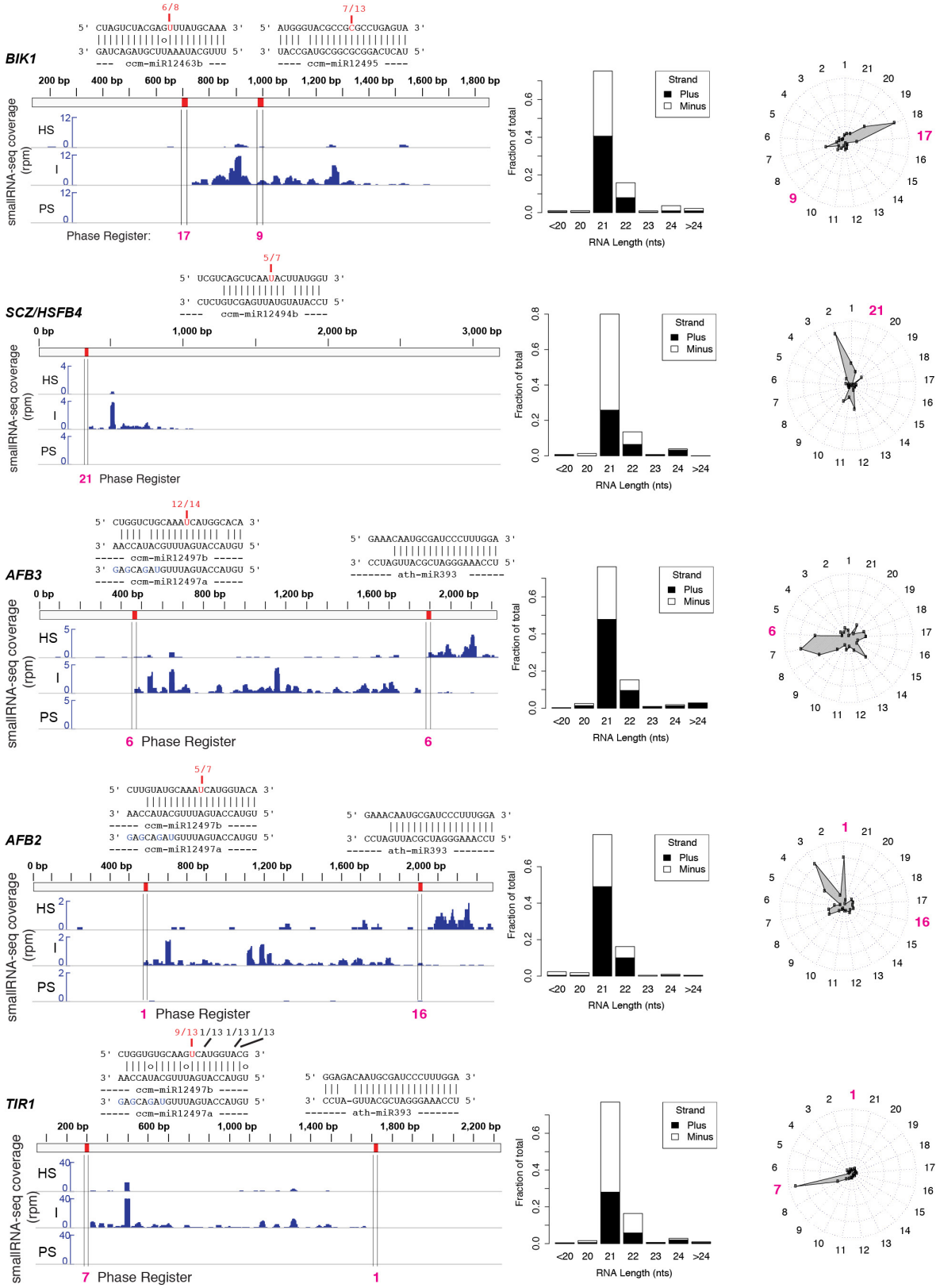


**Extended Data Figure 2 | *C. campestris* miRNAs cause slicing and phased siRNA production from host mRNAs.** Small-RNA-seq coverage across the indicated *A. thaliana* transcripts are shown in blue for host stem, interface, and parasite stem samples. For display, the two biological replicates of each type were merged. Red marks and vertical lines show positions of complementary sites to *C. campestris* miRNAs, with the alignments shown above. Fractions indicate numbers of 5′-RLM-RACE clones with 5′-ends at the indicated positions; the locations in red are the predicted sites for miRNA-directed slicing remnants. Bar charts show the length and polarity distribution of transcript-mapped siRNAs. Radar charts show the fractions of siRNAs in each of the 21 possible phasing registers; the registers highlighted in magenta are those predicted by the miRNA target sites.

```
Cp_v0.1_Contig11111_02898.1 .. A TIR/AFB ortholog
5' CUGGUCUGCAAGUCCUGGUACG 3' Transcript: Cp_v0.1_Contig11111_02898.1:82-103 Slice Site:94
   || ||||o|||o|| ||||||o
3' GAGCAGAUGUUUAGUACCAUGU 5' Query: Cluster_115407_miRNA-star (ccm-miR12497a)

5' CUGGUCUGCAAGUCCUGGUACG 3' Transcript: Cp_v0.1_Contig11111_02898.1:82-103 Slice Site:94
    |||| |||||o|| ||||||o
3' AACCAUACGUUUAGUACCAUGU 5' Query: Cluster_67631_miRNA (ccm-miR12497b)


Cp_v0.1_Contig122651_07831.1 .. A BIK1 ortholog
5' AUGGGUACGCCGCUCCCGAGUA 3' Transcript: Cp_v0.1_Contig122651_07831.1:668-689 Slice Site:680
   |||| |||||||| || |||||
3' UACCGAUGCGGCGCGGACUCAU 5' Query: Cluster_54651_miRNA (ccm-miR12495)


Cp_v0.1_Contig297862_09445.1 .. A TIR/AFB ortholog
5' CUGGUCUGCAAGUCCUGGUACG 3' Transcript: Cp_v0.1_Contig297862_09445.1:82-103 Slice Site:94
   || ||||o|||o|| ||||||o
3' GAGCAGAUGUUUAGUACCAUGU 5' Query: Cluster_115407_miRNA-star (ccm-miR12497a)

5' CUGGUCUGCAAGUCCUGGUACG 3' Transcript: Cp_v0.1_Contig297862_09445.1:82-103 Slice Site:94
    |||| |||||o|| ||||||o
3' AACCAUACGUUUAGUACCAUGU 5' Query: Cluster_67631_miRNA (ccm-miR12497b)


Cp_v0.1_Contig3449_00601.1 ..A TIR/AFB ortholog
5' CUCGUCUGCAAGUCGUGGUACC 3' Transcript: Cp_v0.1_Contig3449_00601.1:259-280 Slice Site:271
   |||||||o|||o||o||||||
3' GAGCAGAUGUUUAGUACCAUGU 5' Query: Cluster_115407_miRNA-star (ccm-miR12497a)

Cp_v0.1_Contig370259_15766.1 .. An SCZ/HSFB4 ortholog
5' CAGACAGCUCAACACAUACGGG 3' Transcript: Cp_v0.1_Contig370259_15766.1:225-246 Slice Site:237
    |||||||||||| ||||| ||o
3' CUCUGUCGAGUUAUGUAUACCU 5' Query: Cluster_57001_miRNA (ccm-MIR12494b)

Cp_v0.1_Contig501179_37185.1 .. An SCZ/HSFB4 ortholog
5' CAGACAGCUCAACACAUACGGG 3' Transcript: Cp_v0.1_Contig501179_37185.1:213-234 Slice Site:225
    |||||||||||| ||||| ||o
3' CUCUGUCGAGUUAUGUAUACCU 5' Query: Cluster_57001_miRNA (ccm-MIR12494b)


Cp_v0.1_Contig70142_36225.1 .. An SCZ/HSFB4 ortholog
5' CAGGCAGCUCAACACUUAUGGA 3' Transcript: Cp_v0.1_Contig70142_36225.1:300-321 Slice Site:312
    ||o|||||||| || ||||||
3' CUCUGUCGAGUUAUGUAUACCU 5' Query: Cluster_57001_miRNA (ccm-MIR12494b)

Cp_v0.1_Contig81842_24454.1 .. A BIK1 ortholog
5' UUGUAUAUGAAUUUAUGCAGA 3' Transcript: Cp_v0.1_Contig81842_24454.1:608-628 Slice Site:619
   |||| ||||||| o|||||||
3' AACAAAUACUUAUGUACGUCU 5' Query: Cluster_105389_miRNA-star (ccm-MIR12463a)

5' CUUGUAUAUGAAUUUAUGCAGA 3' Transcript: Cp_v0.1_Contig81842_24454.1:607-628 Slice Site:619
   || || ||o||||||||||o|
3' GAUCAGAUGCUUAAAUACGUUU 5' Query: Cluster_105391_miRNA (ccm-MIR12463b)

5' AAGGCUAUGCUGCCCCUGAGUA 3' Transcript: Cp_v0.1_Contig81842_24454.1:893-914 Slice Site:905
     |||||o||o|| ||||||||
3' UACCGAUGCGGCGCGGACUCAU 5' Query: Cluster_54651_miRNA (ccm-MIR12495)
```

**Extended Data Figure 3 | Possible miRNA target sites within endogenous *C. campestris* mRNAs.** Note that none of these mRNAs showed evidence of secondary siRNA accumulation, and the complementarity of these sites was generally poor.

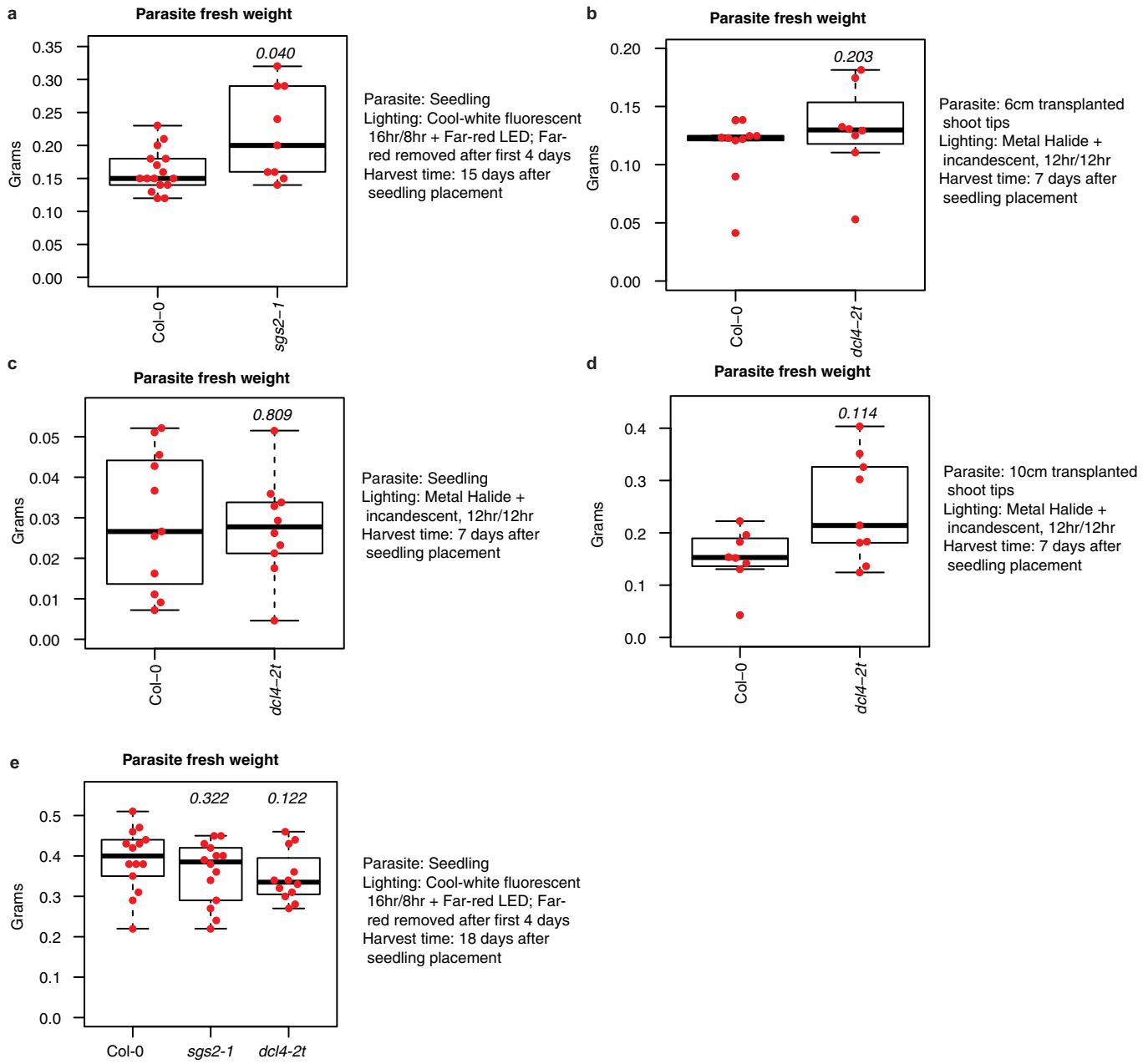


**Extended Data Figure 4 | Growth of *C. campestris* on *A. thaliana sgs2-1* and *dcl4-2t* mutants with varying methodologies, as indicated.** **a**–**d**, *P* values (Wilcoxon rank-sum tests, unpaired, two-tailed) from comparison of mutant to wild-type (Col-0) are shown. Box plots show the median, box edges represent the first and third quartiles, the whiskers extend to 1.5× interquartile range, and all data are shown as dots. **a**, $n = 16$ and 9 biologically independent samples for Col-0 and *sgs2-1*, respectively. 95% confidence interval (Col-0 minus *sgs2-1*), 0.120 to 0.000. **b**, $n = 10$ and 8 biologically independent samples for Col-0 and *dcl4-2t*, respectively. 95% confidence interval (Col-0 minus *dcl4-2t*), −0.052 to 0.012. **c**, $n = 11$ and 10 biologically independent samples for Col-0 and *dcl4-2t*, respectively. 95% confidence interval (Col-0 minus *dcl4-2t*), −0.014 to 0.018. **d**, $n = 8$ and 9 biologically independent samples for Col-0 and *dcl4-2t*, respectively. 95% confidence interval (Col-0 minus *dcl4-2t*), −0.184 to 0.008. **e**, $n = 14$, 14 and 12 biologically independent samples for Col-0, *sgs2-1*, and *dcl4-2t*, respectively. 95% confidence interval (Col-0 minus *sgs2-1*), −0.020 to 0.090. 95% confidence interval (Col-0 minus *dcl4-2t*), −0.010 to 0.110.

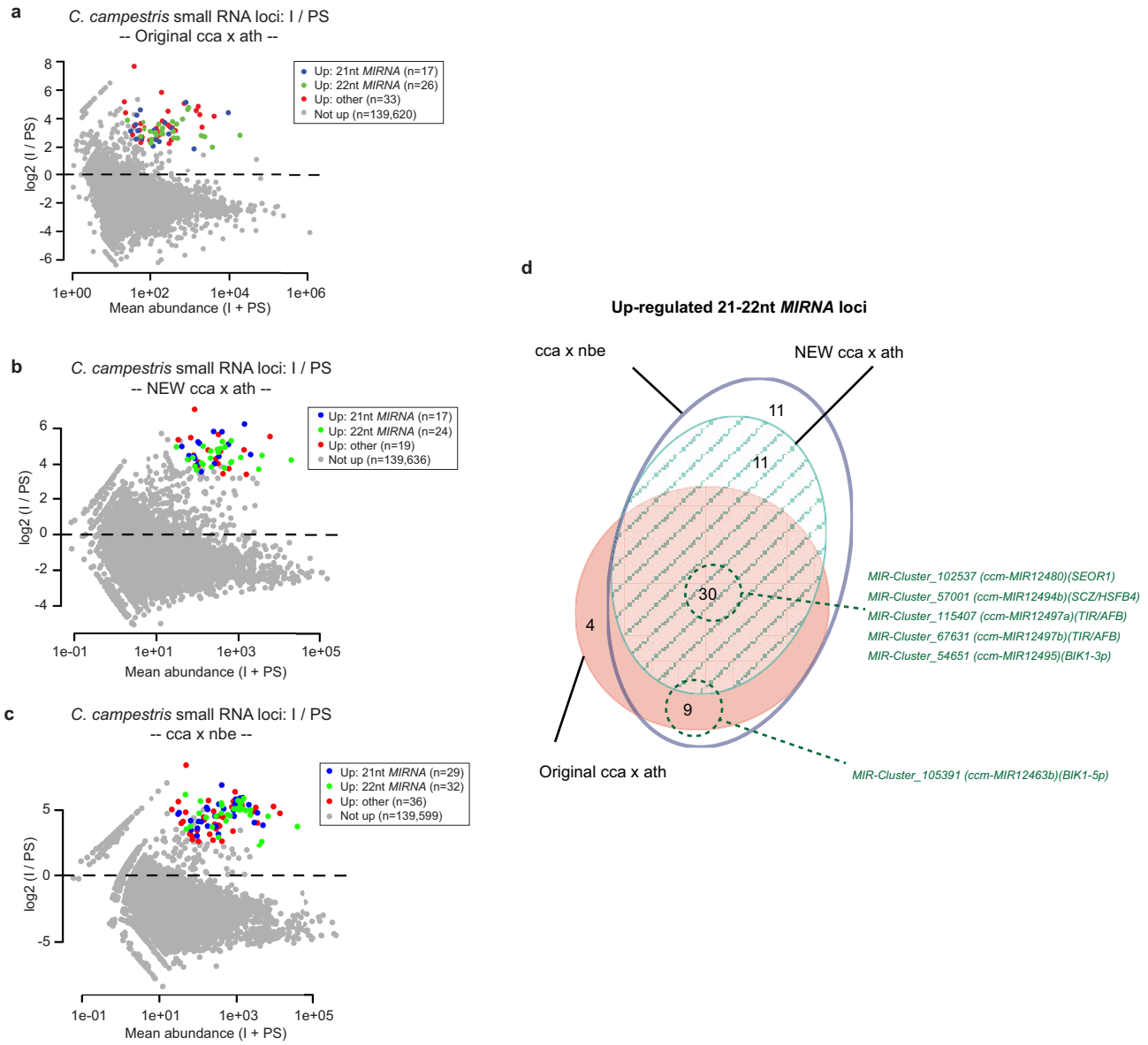


**Extended Data Figure 5 | Highly reproducible induction of *C. campestris* miRNAs in different hosts. a**, Mean abundance plot from original experiment on *A. thaliana* hosts of *C. campestris* small-RNA loci comparing interface to parasite stem samples. Significantly upregulated loci are highlighted (alternative hypothesis: true difference >2-fold, FDR ≤ 0.05 after correction for multiple testing with the Benjamini–Hochberg procedure). Reproduced from Fig. 1a. **b**, **c**, As **a**, except for a new set of *A. thaliana* hosts (**b**) or from an experiment using *N. benthamiana* as hosts (**c**). Significantly upregulated loci are highlighted (alternative hypothesis: true difference > 2-fold, FDR ≤ 0.05 after correction for multiple testing with the Benjamini–Hochberg procedure). **d**, Area-proportional Euler diagram showing overlaps of upregulated *C. campestris* 21–22-nucleotide miRNA loci among the three small-RNA-seq experiments. The locations of the six miRNA loci of special interest are highlighted in green.

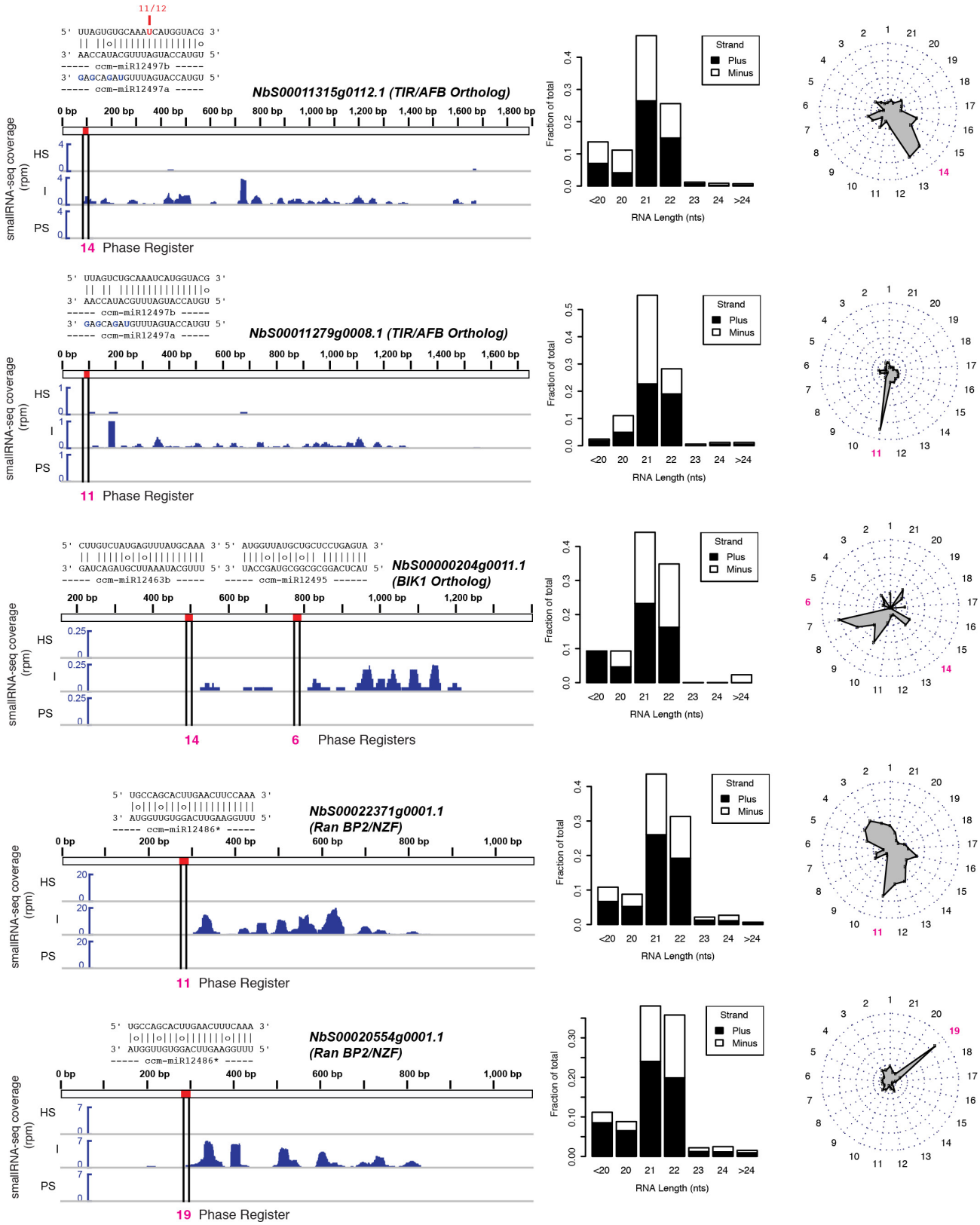


**Extended Data Figure 6 | *C. campestris* miRNAs cause slicing and phased siRNA production from *N.benthamiana* mRNAs.** Small-RNA-seq coverage across the indicated *N. benthamiana* transcripts are shown in blue for host stem, interface, and parasite stem samples. For display, the two biological replicates of each type were merged. Red marks and vertical lines show position of complementary sites to *C. campestris* miRNAs, with the alignments shown above. Fraction indicates numbers of 5′-RLM-RACE clones with 5′-ends at the indicated positions; the locations in red are the predicted sites for miRNA-directed slicing remnants. Bar charts show the length and polarity distribution of transcript-mapped siRNAs. Radar charts show the fractions of siRNAs in each of the 21 possible phasing registers; the registers highlighted in magenta are those predicted by the miRNA target sites.

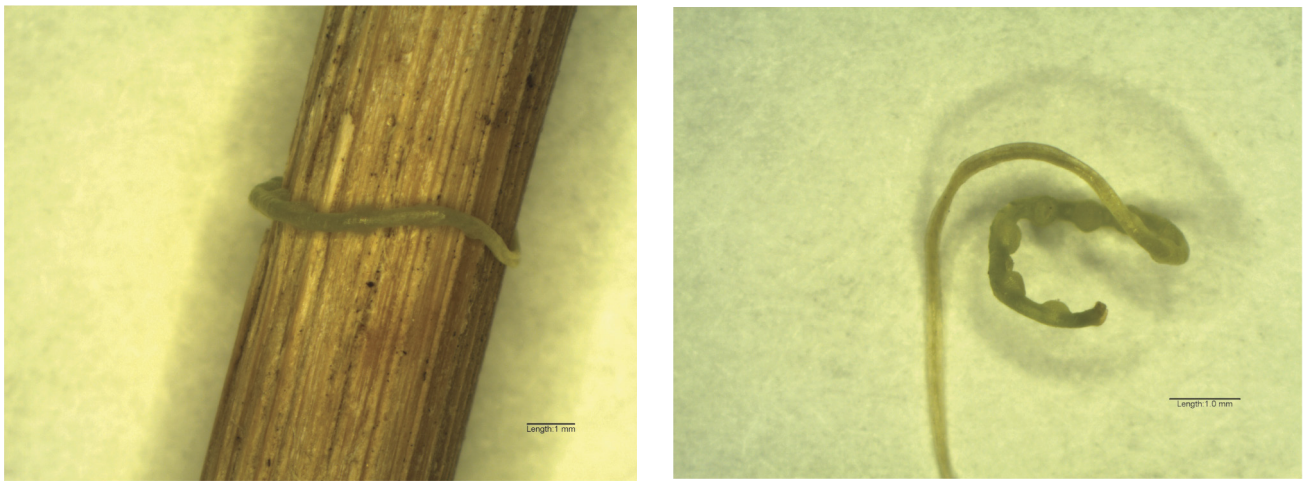


**Extended Data Figure 7 | *C. campestris* pre-haustoria. a**, *C. campestris* seedling wound around a bamboo stake. **b**, The same seedling, removed from the stake to show the prominent pre-haustorial bumps. Seedling was scarified, germinated on moist paper towels for three days at ~28 °C, and then placed next to a bamboo stake for four days with far-red LED lighting. Approximately 30 such seedlings were used for the pre-haustoria RNA in Fig. 4b. Scale bars, 1 mm.

**Extended Data Table 1 | Predicted miRNA targets multiple plant species**

| Phytozome 11 species code | Species | *BIK1* | *SEOR1* | *SCZ / HSFB4* | *TIR1* | *GAPDH* |
|---|---|---|---|---|---|---|
| Org_Acoerulea | *Auilegia coerulea* | 0 | 1 | 0 | 1 | 0 |
| Org_Alyrata | *Arabidopsis lyrata* | 1 | 1 | 0 | 1 | 0 |
| Org_Athaliana | *Arabidopsis thaliana* | 1 | 1 | 1 | 1 | 0 |
| Org_BrapaFPsc | *Brassica rapa* | 1 | 0 | 1 | 1 | 0 |
| Org_Bstricta | *Boechera stricta* | 1 | 0 | 0 | 1 | 0 |
| Org_Cclementina | *Citrus clementina* | 0 | 1 | 0 | 0 | 0 |
| Org_Cgrandiflora | *Capsella grandiflora* | 1 | 0 | 0 | 1 | 0 |
| Org_Cpapaya | *Carica papaya* | 1 | 0 | 1 | 1 | 0 |
| Org_Crubella | *Capsella rubella* | 1 | 0 | 0 | 1 | 0 |
| Org_Csativus | *Cucumus sativus* | 0 | 0 | 0 | 0 | 0 |
| Org_Csinensis | *Citrus sinensis* | 1 | 1 | 0 | 1 | 0 |
| Org_Egrandis | *Eucalyptus grandis* | 0 | 1 | 1 | 1 | 0 |
| Org_Esalsugineum | *Eutrema salsugineum* | 1 | 0 | 0 | 1 | 0 |
| Org_Fvesca | *Fragaria vesca* | 0 | NA | NA | 1 | 1 |
| Org_Gmax | *Glycine max* | 1 | 1 | 1 | 1 | 0 |
| Org_Graimondii | *Gossypium raimondii* | 1 | 0 | 1 | 1 | 0 |
| Org_Kmarnieriana | *Kalanchoe marnieriana* | 0 | 1 | 1 | 1 | 0 |
| Org_Lusitatissimum | *Linum usitatissimum* | 0 | 1 | 0 | 0 | 0 |
| Org_Mdomestica | *Malus domestica* | 0 | NA | 0 | 1 | 0 |
| Org_Mesculenta | *Manihot esculenta* | 1 | 1 | 0 | 1 | 0 |
| Org_Mguttatus | *Mimulus gattus* | 1 | NA | 0 | 1 | 0 |
| Org_Mtruncatula | *Medicago truncatula* | 1 | 1 | 0 | 1 | 0 |
| Org_Ppersica | *Prunus persica* | 0 | NA | 0 | 1 | 0 |
| Org_Ptrichocarpa | *Populus trichocarpa* | 1 | 1 | 1 | 1 | 0 |
| Org_Pvulgaris | *Phaseolus vulgaris* | 0 | 1 | 0 | 1 | 0 |
| Org_Rcommunis | *Ricinus communis* | 1 | 1 | 0 | 1 | 0 |
| Org_Slycopersicum | *Solanum lycopersicum* | 0 | 1 | 1 | 1 | 0 |
| Org_Spurpurea | *Salix purpurea* | 0 | 1 | 1 | 0 | 0 |
| Org_Stuberosum | *Solanum tuberosum* | 1 | NA | 1 | 1 | 0 |
| Org_Tcacao | *Theobroma cacao* | 0 | 1 | 1 | 1 | 0 |
| Org_Vvinifera | *Vitis vinifera* | 0 | 1 | 1 | 1 | 0 |

Targets were predicted using targetfinder.pl, keeping all hits with a score of 4.5 or less. Probable orthologues of the indicated *A. thaliana* genes were found using BLASTP against the 31 eudicot species present in Phytozome 11, simply keeping up to the top 100 BLAST hits. miRNA queries were all mature miRNA and miRNA* from *C. campestris* interface-induced miRNA loci. NA, indicates that no probable orthologues were recovered from a given species; 1, indicates that there was one or more predicted target in that species; 0, indicates there were 0 predicted targets. GAPDH orthogroup, negative control.